In the Proceedings of the 1989 IEEE Conference on Decision and Control in Tampa, FL, December 1989.

Identification of Sampled Data Systems at Frequencies Beyond the Nyquist Rate

Rick Ehrlich*
NeXT, Inc.
900 Chesapeake Dr.
Redwood City, CA 94063
Phone: (415) 366-0900

Carl Taussig
Hewlett-Packard Laboratories
1501 Page Mill Road, M/S 2U
Palo Alto, CA 94304
Phone: (415) 857-4258

Daniel Abramovitch
Hewlett-Packard Laboratories
1501 Page Mill Road, M/S 2U
Palo Alto, CA 94304
Phone: (415) 857-3806

Abstract— **This paper proposes a practical algorithm for identifying the dynamics of a continuous-time linear, time-invariant system, embedded in a sampled feedback loop with fixed sample time, T. We will show that if the closed-loop configuration is stable, it is rather straightforward to design a set of experiments using a spectrum analyzer that will identify the plant transfer function, $G_p(j\omega)$, to frequencies well beyond the Nyquist frequency, $\omega_N = \frac{\pi}{T}$. Experimental results are included.**

I. Introduction

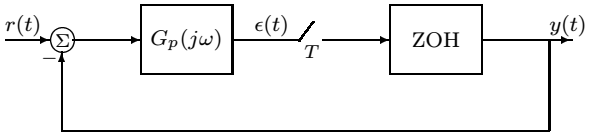

Figure 1: Closed-loop sampled data system.

In this paper, we examine the identification of the dynamics of a sampled-data system, as shown in Fig. 1, at frequencies above the Nyquist frequency, $\omega_N = \frac{\pi}{T}$, where T is the time between samples [1]. The configuration that we will study is a common configuration where both the plant and the controller are continuous[1], but the output of the plant is only sampled every T seconds.

This type of sampled data system has been studied as far back as Ragazzini and Zadeh [2]. In general, the analysis of such systems has been carried out with the assumption that T was small enough such that $|G_p(j\omega)|$ was negligibly small for $\omega \geq \frac{\pi}{T}$, the Nyquist frequency. This paper deals with the identification of dynamics of $G_p(j\omega)$ above the Nyquist frequency. We will show that if the closed-loop configuration is stable, it is rather straightforward to design a set of experiments using a spectrum analyzer[2] that will identify $G_p(j\omega)$ to arbitrarily high frequencies[3]. This work can be considered to be an extension of the relatively well known off-line, non-parametric algorithms for identification of the dynamics of a continuous-time system embedded in an analog feedback loop from transfer function measurements of the closed-loop system [3]. This is in contrast to recent results in the identification of a plant embedded in a multi-rate digital control system, which extend well known on-line, parametric techniques [4, 5].

I.A Overview

The rest of the paper will proceed as follows. Section II presents some background material on the Sampling Theorem and its extensions. Section III presents a brief derivation of the formulae necessary to determine the continuous-time transfer function of a linear, time-invariant (LTI) system that is embedded in a sampled control-loop from measurements of the response characteristics of the overall control-loop. The problem is formally described in Sec. III.A. Because the sampler is the source of most of the difficulties in the analysis of the situation, Sec. III.B is devoted to a discussion of the properties of sampled signals within the control-loop. The equations constraining the overall control-loop are stated in Sec. III.C and solved to relate the spectra of the system input and output in the general case. Section III.D considers two special case inputs for which the system response is particularly simple, and Sec. III.E proposes a procedure for determining the plant transfer function, $G_p(j\omega)$, from the response of the closed-loop system to a series of single-frequency inputs. A test case of the procedure is presented in Sec. IV and these results are discussed in Sec. V.

II. Background

The fundamental work on sampling was done by Nyquist [6] and popularized by Shannon [1]. The Sampling Theorem, simply stated, says that in order to recover a bandlimited signal with its highest frequency component at f_c, the sampler must be run at $f_s = \frac{1}{T} \geq 2f_c$. The basic assumption here is that the signal is low-pass. In contrast, we will

*The work reported in this paper was performed by the authors at Hewlett-Packard Laboratories.

[1] Here lumped together in $G_p(j\omega)$.

[2] For example, an HP 3562A Dynamic Signal Analyzer.

[3] Bounded only by the bandwidth of the spectrum analyzer, not the control system.

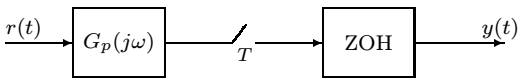

Figure 2: Open-loop sampling.

assume that we have a narrowband signal ($BW \ll 2f_c$), but that the band center is not necessarily at $f = 0$ and in fact will often be above f_s.

II.A Previous Extensions of the Sampling Theorem

The basic Nyquist sampling theorem was extended by Linden [7] to include the interlaced sampling of two samplers whose sample intervals are shifted in time by some number α. For $\alpha \neq nT$ (n an integer), the effective Nyquist frequency is raised. If the output of the system, $y(t)$ in Fig. 2, is periodic *i.e.,* $y(t) = y(t + \tau)$, and if $T \neq n\tau$, then the same effect can be achieved by retaining the previous samples of $y(t)$ and adding the new samples (which are shifted in time by the fact that $T \neq \tau$). Sampling oscilloscopes make use of this principle to sample periodic functions that have frequency content above the Nyquist rate of the oscilloscope based upon a single sampler[8]. Note that the only assumption made about the waveform measured by the oscilloscope is that it must be periodic.

II.B Sinusoidal Input to LTI System with Sampled Output

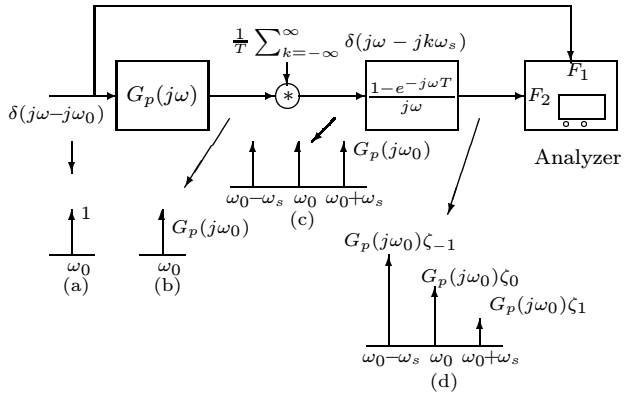

Figure 3: Sinusoidal input to LTI system with sampled output. Here $\zeta_n = \left[\frac{1-e^{-j(\omega_0+n\omega_s)T}}{j(\omega_0+n\omega_s)T}\right]$, and an "$*$" symbolizes convolution. Note that this is a plot of frequency domain quantities.

On the other hand, if we assume that $u(t)$ consists of a single complex sinusoid *i.e.,* $u(t) = e^{j\omega_0 t}$, then we know that $y(t)$, having been passed through a linear, time-invariant filter, will also be a complex sinusoid at the same frequency. Only the phase and the magnitude will be altered by G_p yielding $y(t) = G_p(j\omega_0)e^{j\omega_0 t}$. The frequency domain representation of this is depicted in Fig. 3. The single, complex sinusoid Fourier transforms to a Dirac Delta function, (a). Passing through G_p modifies the phase and magnitude, (b). Sampling in time transforms to convolution with a series of Delta functions in frequency, thus replicating the impulses at $\omega_0 + n\omega_s$ where n is an integer and ω_s is the sample frequency, (c). These samples are filtered as they pass through the zero-order hold, again modifying their gain and phase, (d).

The block marked, "Analyzer", in Fig. 3 computes the ratio of the cross-spectrum of its two inputs to the auto-spectrum of one of them,

$$H_{eff}(j\omega) \equiv \frac{F_2(j\omega)\overline{F}_1(j\omega)}{F_1(j\omega)\overline{F}_1(j\omega)} \tag{1}$$

where $\overline{F}_1(j\omega)$ is the complex conjugate of $F_1(j\omega)$, and $F_1(j\omega)$ and $F_2(j\omega)$ are the two inputs of the analyzer. For the system of Fig. 3, the single-frequency system input is applied to the first input of the analyzer, and the output of the zero-order hold is applied to the second input. Thus, $F_1(j\omega)$ and $F_2(j\omega)$ are as plotted in (a) and (d), respectively, of Fig. 3. The value of $H_{eff}(j\omega_\circ)$ is then[4]

$$H_{eff}(j\omega_\circ) = G_p(j\omega_\circ)\frac{1 - e^{-j\omega_\circ T}}{j\omega_\circ T} \tag{2}$$

From here, it is straightforward to extract $G_p(j\omega_0)$. In this case, the effective transfer function $H_{eff}(j\omega_\circ)$ can be thought of as the ratio between the output and input spectral amplitudes at the excitation frequency, $\omega_\circ$. It is not an actual continuous-time transfer function because the action of the sampler makes the overall system time-varying.

III. Theory

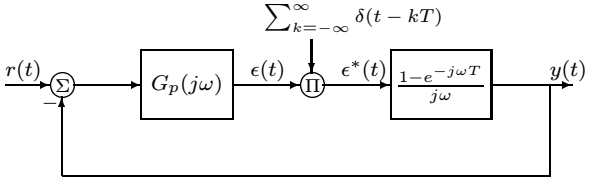

Figure 4: Closed-loop sampled data system.

[4]Computation of $H_{eff}(j\omega)$ with the inputs described here involves multiplication of two impulse-functions at $\omega = \omega_\circ$ in each of the numerator and denominator of the fraction in Eq. (1). The product of two co-incident impulses is not defined. However, if the unit impulse at $\omega_\circ$ is replaced by a narrow pulse of unity area, centered at $\omega = \omega_\circ$, then the problem of computing $H_{eff}(j\omega_\circ)$ is well posed. The situation presented here can be considered to be the limiting case of an input-spectrum consisting of a very narrow unity-area pulse at $\omega = \omega_\circ$.

III.A Problem Statement

The closed-loop system is modelled as pictured in Fig. 4. It is assumed that the closed-loop system is stable in the sense that bounded inputs produce bounded outputs[9]. The system input, $r(t)$, is assumed to be completely controlled (and thus, known) by the experimenter. The only system output that the experimenter can observe, however, is the sampled output, $y(t)$. The transfer function of the LTI system under test is $G_p(j\omega)$. The sample-hold is represented by a multiplier, which modulates the incoming signal by an infinite train of unit-area impulses, spaced in time by T, followed by a zero-order hold function, $G_h(j\omega)$:

$$G_h(j\omega) \equiv \frac{1 - e^{-j\omega T}}{j\omega} \quad . \tag{3}$$

III.B Properties of Impulse-Modulated Signals

Although it is not physically accessible in an actual system, it is of interest to consider the signal immediately after the multiplier, labeled $\epsilon^*(t)$ in Fig. 4. Using notation developed in Franklin and Powell[9], $\epsilon^*(t)$ is defined,

$$\epsilon^*(t) \equiv \sum_{k=-\infty}^{+\infty} \epsilon(t)\delta(t - kT) \tag{4}$$

where $\delta(t)$ is the Dirac Delta function [10]. In this section, it will be assumed that appending the "star" superscript, " *", to any time-domain quantity implies modulation of that quantity in the manner prescribed by (4), and that appending a "star" to a frequency-domain quantity implies that the Fourier transform of the appropriately modulated corresponding time-domain quantity is to be taken. For example, since $E(j\omega)$, the Fourier transform of $\epsilon(t)$, is defined,

$$E(j\omega) \equiv \int_{-\infty}^{+\infty} \epsilon(t)e^{-j\omega t}dt \tag{5}$$

the convention of this section requires that

$$E^*(j\omega) = \int_{-\infty}^{+\infty} \epsilon^*(t)e^{-j\omega t}dt \quad . \tag{6}$$

Using Eqs. (4) – (6), several properties of the "star"-ed frequency-domain quantities can be derived [9].

$$E^*(j\omega) = \frac{1}{T} \sum_{k=-\infty}^{+\infty} E[j(\omega - k\omega_s)] \quad , \tag{7}$$

where

$$\omega_s \equiv \frac{2\pi}{T} \quad . \tag{8}$$

Equation (7) is depicted in Fig. 5, which shows the result of modulation of a band-limited signal. The effect of the modulator is to replicate the signal spectrum at frequency intervals of the sample frequency, ω_s:

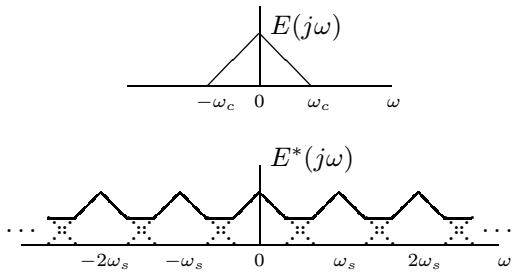

Figure 5: Spectrum of a bandlimited signal modulated by an infinite impulse train.

$$[G(j\omega)\,(E^*(j\omega))]^* = (G^*(j\omega))\,(E^*(j\omega)) \quad . \tag{9}$$

Equation (9) can be thought of as a distributive law for the "star" operator, and can be proven via a straightforward application of (7). Furthermore, $E^*(j\omega)$ is periodic with period ω_s *i.e.,*

$$E^*[j(\omega - n\omega_s)] = E^*(j\omega); \text{ for } n \text{ integer} \quad . \tag{10}$$

Finally, the Fourier transform of $\epsilon^*(t)$ is related to the $\mathcal{Z}$-transform of the sampled signal, $\epsilon(kT)$; k integer by

$$E^*(j\omega) = E_d(z)\,|_{z=e^{j\omega T}} \quad , \tag{11}$$

where

$$E_d(z) \equiv \sum_{k=-\infty}^{+\infty} \epsilon(kT)z^{-k} \quad . \tag{12}$$

This fact is useful in interpreting the results of analyses presented later in this section.

III.C System Analysis

From Fig. 4, two constraints relating $Y(j\omega)$, $E(j\omega)$, and $R(j\omega)$ can be derived:

$$E(j\omega) = G_p(j\omega)\,[R(j\omega) - Y(j\omega)] \tag{13}$$

and

$$Y(j\omega) = G_h(j\omega)\,[E^*(j\omega)] \quad . \tag{14}$$

Substituting for $Y(j\omega)$ from (14) into (13) and "star"-ing both sides yields:

$$E^*(j\omega) = [G_p(j\omega)R(j\omega)]^* - [G_p(j\omega)G_h(j\omega)\,[E^*(j\omega)]]^* \, . \tag{15}$$

Equation (15) can be simplified by application of (9) and then solved for $E^*(j\omega)$:

$$E^*(j\omega) = \frac{[G_p(j\omega)R(j\omega)]^*}{1 + [G_p(j\omega)G_h(j\omega)]^*} \quad . \tag{16}$$

Finally, (14) can be substituted into (16) to give an expression relating $Y(j\omega)$ and $R(j\omega)$, the output and input, respectively, of the closed-loop system:

$$Y(j\omega) = \frac{G_h(j\omega)\left[G_p(j\omega)R(j\omega)\right]^*}{1+\left[G_p(j\omega)G_h(j\omega)\right]^*} \quad . \tag{17}$$

Note that there is no way to manipulate Eq. (17) so as to provide a ratio between $Y(j\omega)$ and $R(j\omega)$ (*i.e.,* a transfer function for the closed-loop system). This is impossible, because the system is **not** LTI[5].

III.D Special-Case Inputs

There are two special inputs for which the system response can be easily determined. These two special cases are examined in the sub-sections below in order to provide further insight into the behavior of the system of Fig. 4.

III.D.1 Unit Pulse Input

For the first special case, the input, $r_1(t)$, will be assumed to be a unit pulse of duration, T, which begins and ends at sample-instants. The Fourier transform of such an input is

$$R_1(j\omega) = \frac{1-e^{-j\omega T}}{j\omega} \tag{18}$$

It should be noted that the input spectrum, $R_1(j\omega)$, is identical to the transfer function of the zero-order hold, $G_h(j\omega)$. Substituting $R_1(j\omega)$ for $R(j\omega)$ in Eq. (16), and recognizing that $R_1(j\omega) = G_h(j\omega)$ yields

$$E_1^*(j\omega) = \frac{\left[G_p(j\omega)G_h(j\omega)\right]^*}{1+\left[G_p(j\omega)G_h(j\omega)\right]^*} \tag{19}$$

where $E_1(j\omega)$ represents the value of $E(j\omega)$ for the case when $R(j\omega) = R_1(j\omega)$.

Now, as was stated in Eq. (11), the spectrum, $E^*(j\omega)$ is equal to the Z-transform of the sampled sequence, $\epsilon(kT)$, evaluated at $z = e^{-j\omega T}$. Since the only elements between $\epsilon(t)$ and $y(t)$ in Fig. 4 are those that make up the sample/hold device, it is seen that

$$y(kT) = \epsilon(kT); \quad k \text{ integer.} \tag{20}$$

Thus, the right-hand side of Eq. (19) also represents the Z-transform of the output-sequence, $y_1(kT)$, evaluated at $z = e^{-j\omega T}$. Since the input, $r_1(t)$, is a unit pulse, the right-hand side of Eq. (19) is actually the discrete-time transfer function for the closed-loop system, defined for inputs that change only at sample-instants.

III.D.2 Single-Frequency Input

The second special case to be considered here is that of a single-frequency input of amplitude, R_o, and complex frequency, $s = j\omega_o$:

$$R_2(j\omega) = R_o\delta(\omega-\omega_o). \tag{21}$$

For this special case, Eq. (17) can be manipulated to provide a quantity that has many of the properties of a continuous-time transfer function for the closed-loop system. Substituting $R_2(j\omega)$ for $R(j\omega)$ in Eq. (17), using Eq. (7), and considering only frequencies near $\omega = \omega_o$, gives

$$Y_2(j\omega) = \frac{G_p(j\omega)G_h(j\omega)}{1+\left[G_p(j\omega)G_h(j\omega)\right]^*}R_o\frac{1}{T}\delta(\omega-\omega_o); \tag{22}$$

for $\mid \omega-\omega_o \mid < \omega_s$. Equation (22) can be re-expressed as

$$Y_2(j\omega) = Y_o\delta(\omega-\omega_o); \quad \mid \omega-\omega_o \mid < \omega_s \tag{23}$$

where

$$Y_o \equiv \frac{G_p(j\omega_o)G_h(j\omega_o)}{1+\left[G_p(j\omega_o)G_h(j\omega_o)\right]^*}R_o\frac{1}{T} \; . \tag{24}$$

The quantity, Y_o, can be thought of as the Fourier component of $y_2(t)$ at the excitation frequency, ω_o. The effective transfer function, $H_{eff}(j\omega)$, was argued in Sec. II to be equal to the ratio between the output and input spectral amplitudes at the excitation frequency, $\omega_\circ$. With the system output and input being defined as $Y(j\omega)$ and $R(j\omega)$, respectively,

$$H_{eff}(j\omega) = \frac{Y_o}{R_o} = \frac{G_p(j\omega)G_h(j\omega)}{1+\left[G_p(j\omega)G_h(j\omega)\right]^*}\cdot\frac{1}{T} \; . \tag{25}$$

Note that $H_{eff}(j\omega)$ is unitless, with the units of $G_h(j\omega)$ cancelling those of the $\frac{1}{T}$ in Eq. (25).

The effective transfer function, $H_{eff}(j\omega)$, is significant because it is a relatively easy quantity to measure for an actual system, as was argued in Sec. II. It will be shown in this section that such measurements can be used to determine $G_p(j\omega)$, the continuous-time transfer function of the LTI system under test.

A small amount of algebraic manipulation must be performed in order to solve Eq. (25) for $G_p(j\omega)G_h(j\omega)$ in terms of $H_{eff}(j\omega)$. For convenience, the unitless quantity, $H_\Sigma(j\omega)$, is defined.

$$\begin{aligned} H_\Sigma(j\omega) & \\ &\equiv \sum_{k=-\infty}^{+\infty} H_{eff}(j[\omega-k\omega_s]) \qquad (26)\\ &= \sum_{k=-\infty}^{+\infty} \frac{G_p(j[\omega-k\omega_s])G_h(j[\omega-k\omega_s])}{1+\left[G_p(j[\omega-k\omega_s])G_h(j[\omega-k\omega_s])\right]^*}\cdot\frac{1}{T} \; . \end{aligned}$$

Equation (10) can be used to simplify the denominator of (26), and Eq. (7) can be applied to the summation in the numerator, yielding

$$H_\Sigma(j\omega) = \frac{\left[G_p(j\omega)G_h(j\omega)\right]^*}{1+\left[G_p(j\omega)G_h(j\omega)\right]^*} \quad . \tag{27}$$

Note that the expression for $H_\Sigma(j\omega)$ in Eq. (27) is exactly equal to the right-hand side of Eq. (19). Thus, $H_\Sigma(j\omega)$ is simply the discrete-time transfer function of the closed-loop system, evaluated at $z = e^{j\omega T}$.

[5] It is linear, but it is not time-invariant.

Equation (27) can be solved for $[G_p(j\omega)G_h(j\omega)]^*$, and the result substituted into Eq. (25) to yield an expression for $[G_p(j\omega)G_h(j\omega)]$ in terms of $H_{eff}(j\omega)$ and $H_\Sigma(j\omega)$:

$$G_p(j\omega)G_h(j\omega)\cdot\frac{1}{T}=\frac{H_{eff}(j\omega)}{1-H_\Sigma(j\omega)}\quad . \tag{28}$$

III.E Measurement Procedure

Given an infinite set of measured values for $H_{eff}(j\omega), \omega\in[-\infty,+\infty]$, one could, in principle, compute $H_\Sigma(j\omega)$ for all $\omega\in[-\infty,+\infty]$ via an infinite summation, as prescribed in Eq. (7).

$$H_\Sigma(j\omega)=\sum_{k=-\infty}^{+\infty}H_{eff}[j(\omega-k\omega_s)]\quad . \tag{29}$$

In a practical situation, however, measurements can be taken only at a limited number of points so that the summation of Eq. (29) must be truncated after a finite number of terms. Thus, it is of interest to know how many terms should be included (and indeed, whether the summation converges at all!).

Since the closed-loop system is stable, the discrete-time closed-loop transfer function must be finite for all $z\in[z:|z|=1]$. Thus, because $H_\Sigma(j\omega)$ is equal to the discrete-time transfer function of the closed-loop system, evaluated at $z=e^{j\omega T}$, $H_\Sigma(j\omega)$ must be finite for all real ω.

The number of terms of Eq. (29) that must be included to insure an accurate estimate of $H_\Sigma(j\omega)$ is difficult to determine in general. A reasonable algorithm would be to include enough terms so that the last few terms taken together add insignificantly to the summation. Given measurements of $H_{eff}(j\omega)$ over a limited range of frequencies, $H_\Sigma(j\omega)$ would thus be estimated by

$$H_\Sigma(j\omega)\simeq\sum_{k=-N}^{+N}H_{eff}[j(\omega-k\omega_s)]\quad . \tag{30}$$

This estimated value for $H_\Sigma(j\omega)$ can be used in Eq. (28), along with the measured values of $H_{eff}(j\omega)$, and the formula for $G_h(j\omega)$ in Eq. (3), to estimate $G_p(j\omega)$.

IV. Experimental Verification

This section will report the design and results of an experiment wherein the analysis of Sec. III was applied to a test circuit of the topology depicted in Fig. 1. The measurements reported in this section were all made using an HP 3562A Dynamic Signal Analyzer. This instrument performs frequency-domain, dynamic signal analysis spanning the frequency span from 125 μHz to 100 KHz with a dynamic range greater than 80 dB [11].

The plant selected for the test circuit consists of an op-amp realization of a two pole low pass filter whose transfer function is well represented by the equation

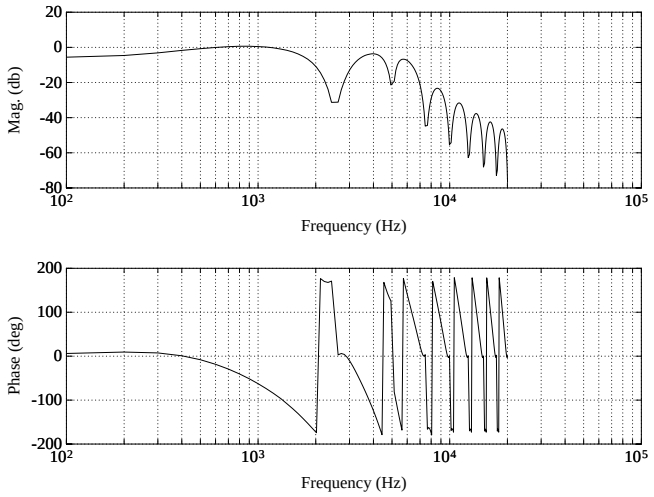

Figure 6: Unprocessed frequency response data from closed-loop system.

$$G_p(j\omega)=\left.\frac{1}{s^2+2\zeta\omega_n s+\omega_n^2}\right|_{s=j\omega}$$
$$=\frac{1}{(\omega_n^2-\omega^2)+2\zeta\omega_n j}\quad . \tag{31}$$

The dimensionless damping ratio ζ, and the natural frequency ω_n are variable parameters of the circuit. The sampler and the zero-order hold are implemented with an Analog Devices AD585 analog sample hold circuit. The AD585 is a monolithic device with a 3.0 μS acquisition time (settle

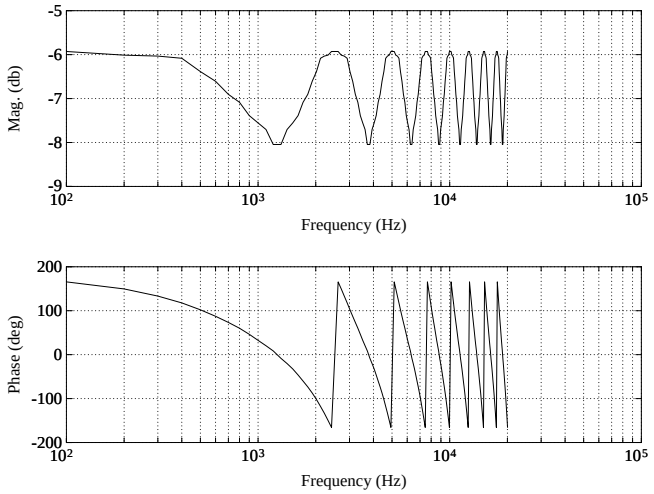

Figure 7: Estimated closed-loop unit pulse response ($\hat{H}_\Sigma(j\omega)$).

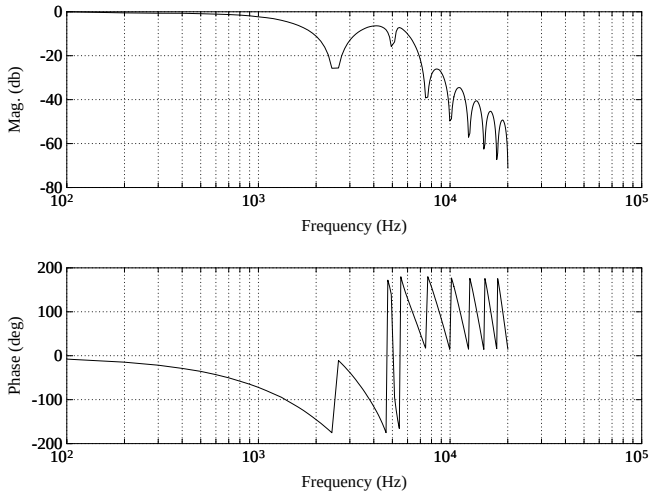

Figure 8: Estimate of transfer function of open-loop plant convolved with zero-order hold and normalized by the sample period ($\hat{G}_p(j\omega)\hat{G}_h(j\omega)\frac{1}{T}$).

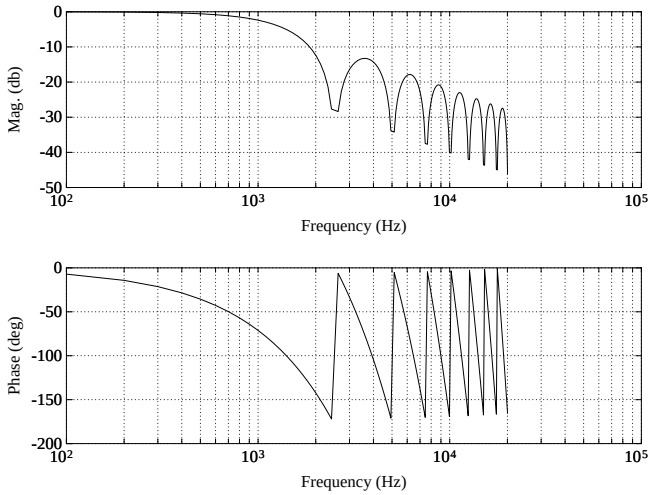

Figure 9: Tranfer function of zero-order hold normalized by sample period ($G_h(j\omega)\frac{1}{T}$).

to 0.01%) and a very low droop rate of 1.0 mV/mS. The sample rate is controlled by an external function generator and is an additional variable parameter of the experiment. As shown in Fig. 1 the output of the sample-hold is inverted and summed with the system's input.

As discussed in Sec. II, the 3562A Dynamic Signal Analyzer has a mode of operation wherein it provides a sinusoidal excitation at a fixed frequency to a system under test and measures the system's response *at that frequency.* In order to reduce the effects of noise, a number of such measurements are averaged. The resulting ratio of the output spectrum to the input spectrum is referred to as the frequency response (at the frequency of the excitation). In the experiments performed on the circuit in Fig. 1, the sinusoidal input was applied at r and the response measured at y. For this circuit, the measurement performed results in the quantity defined as the effective transfer function $H_{eff}(j\omega)$, defined by Eq. (25).

IV.A Experimental Procedure

First, a primary frequency, $\omega_\circ$, is chosen with $\omega_\circ \in \left[-\frac{\omega_s}{2}, \frac{\omega_s}{2}\right]$. The effective transfer function, $H_{eff}(j\omega)$ is measured at $\omega = \omega_\circ$, along with $2N$ other frequencies specified by $\omega = \omega_\circ \pm k\omega_s$, $k = 1 \ldots N$. The effective transfer functions are summed as prescribed by Eq. (30) to provide an approximation to $H_\Sigma(j\omega_\circ)$;

$$\hat{H}_\Sigma(j\omega_\circ) \equiv \sum_{k=-N}^{N} H_{eff}(j\omega_\circ - k\omega_s) \quad . \tag{32}$$

$H_\Sigma(j\omega_\circ)$ is periodic in frequency with period, ω_s. Therefore, the approximation made above provides $\hat{H}_\Sigma(j\omega)$ for $\omega = \omega_\circ - k\omega_s$, $k = -N \ldots N$ not just the primary frequency. Eq. (28) can now be used to extract an estimate of the product $G_p(j\omega)G_h(j\omega)\frac{1}{T}$ for those same frequencies. Finally,

$$\hat{G}_p(j\omega) = \frac{H_{eff}(j\omega)}{1 - \hat{H}_\Sigma(j\omega)} \cdot \frac{T}{G_h(j\omega)} \quad . \tag{33}$$

This procedure can be repeated for an arbitrary number of frequencies in the range $\omega_\circ \in \left[-\frac{\omega_s}{2}, \frac{\omega_s}{2}\right]$.

IV.B Experimental Results

The results presented in this section show the use of the algorithm to identify a lightly damped resonance at a frequency approximately four times the Nyquist frequency ($\zeta \sim .05$, $\omega_n \sim$ 5KHz, $\omega_s \sim$ 2.5KHz). Fig. 6 shows the measurements of $H_{eff}(j\omega)$ for frequencies up to 20 KHz. Fig. 7 is the spectrum, $\hat{H}_\Sigma(j\omega)$, estimated by the sixteen terms provided by the raw data. The estimated open-loop transfer function $\hat{G}_p(j\omega)\hat{G}_h(j\omega)\frac{1}{T}$ extracted from the closed-loop measurements is shown in Fig. 8. The spectrum of Fig. 8 can be divided by the spectrum of the normalized zero-order hold function calculated by the equation,

$$G_h(j\omega)\frac{1}{T} = \frac{1 - e^{-j\omega T}}{j\omega T} \quad , \tag{34}$$

and shown in Fig. 9, resulting in the estimated plant transfer function $\hat{G}_p(j\omega)$. The plant transfer function derived as described above is plotted along with a direct measurement of the filter's frequency response, $G_p(j\omega)$, made with the filter removed from the feedback loop in Fig. 10.

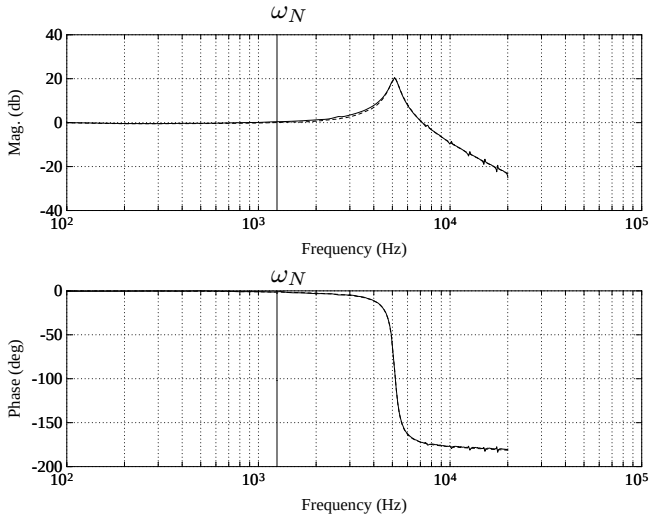

Figure 10: Comparison of algorithm (dashed line) with open-loop plant measurement. The vertical bars indicate the Nyquist frequency of the closed-loop system.

V. Discussion

The agreement between the magnitude plots of $\hat{G}_p(j\omega)$ and $G_p(j\omega)$ in the upper portion of Fig. 10 is such that the two curves are nearly indistinguishable. The same is true of the phase-plots in the lower portion of that figure. A direct measurement of $G_p(j\omega)$, with the plant removed from the sampled control-loop, is certainly much simpler to perform than the technique proposed in this paper. However, for a situation in which the plant cannot be removed from the sampled control-loop and for which the continuous-time plant output is not available, the experimenter requiring data on the high-frequency characteristics of the plant has little choice but to follow the procedure of Sec. IV.

An example of such a situation is the head positioning system for a Winchester disk drive using sectored servo-code[6]. The output of the plant (in this case, the actuator arm position) is available only at discrete times and the system is linear only when it is under closed-loop control near the center of a data track. If the experimenter has continuous-time control of the system input, then the technique outlined here can be used to measure the continuous-time open-loop transfer function of the actuator plus the compensating electronics. In addition, the computed quantity, $\hat{H}_\Sigma(j\omega)$, gives the experimenter an estimate of the discrete-time closed-loop transfer function of the sampled control-loop, as discussed in Sec. III. The discrete-time closed-loop transfer function provides useful information about the stability of the closed-loop system.

[6] Often called embedded servo-code.

REFERENCES

[1] C. E. Shannon, "Communication in the presence of noise," *Proceedings of the IRE*, pp. 10–21, January 1949.

[2] J. Ragazzini and L. Zadeh, "The analysis of sampled-data systems," *Transactions of the AIEE*, pp. 225–234, November 1952.

[3] Hewlett-Packard Application Note, "Control system development using dynamic signal analyzers," Tech. Rep. 243-2, Hewlett-Packard, 1984.

[4] W. Lu and G. Fisher, "Least-squares output estimation with multirate sampling," *IEEE Trans. Aut. Control*, vol. 34, pp. 669–672, June 1989.

[5] W. Lu, D. G. Fisher, and S. L. Shah, "Least-squares output estimation with multirate sampling," in *Proc. American Control Conf.*, (Pittsburg, PA), pp. 1879–1885, June 1989.

[6] H. Nyquist, "Certain factors affecting telegraph speed," *Bell Systems Technical Journal*, vol. 3, p. 324, April 1924.

[7] D. A. Linden, "A discussion of sampling theorems," *Proceedings of the IRE*, pp. 1219–1226, July 1959.

[8] K. Rush and D. J. Oldfield, "A data acquisition system for a 1 GHz digitizing oscilloscope," *Hewlett-Packard Journal*, vol. 37, p. 4, April 1986.

[9] G. F. Franklin and J. D. Powell, *Digital Control of Dynamic Systems*. Menlo Park, California: Addison-Wesley, 1980.

[10] R. N. Bracewell, *The Fourier Transform and Its Applications*. New York: McGraw-Hill, 2 ed., 1978.

[11] J. S. Epstein, G. R. Engel, D. R. Hiller, J. Glen L. Purdy, B. C. Hoog, and E. J. Wicklund, "Hardware design for a dynamic signal analyzer," *Hewlett-Packard Journal*, vol. 35, pp. 12–17, December 1984.